Journal of Aircraft, Vol. 52, No. 6
(2015), pp. 1729-1735.
DOI: 10.2514/1.C033473

Design and numerical modelling of a pressurized airframe bulkhead joint

Ioannis K. Giannopoulos[1]*
Cranfield University, Cranfield, MK43 0AL, UK

Efstathios E. Theotokoglou[2]
National University of Athens, Athens, 157 73, Greece

and
Xiang Zhang[3]
Coventry University, Coventry, CV1 5FB, UK

Abstract

The structural loading on a conceptual lap joint in the empennage of a civil aircraft has been investigated. The lap joint interfaces the end-pressure-part-hemispherical-bulkhead to the cylindrical fuselage. The pressure bulkhead is made of CFRP materials. The aim of the study is to present numerical results of the induced structural loading from the fuselage positive internal pressure differential and the localized high stress intensity field at the lap joint location. A methodology for the appropriate numerical approach to analyze the domed pressure bulkhead is presented. The results of the numerical investigation showed that the laminate loading levels calculated by the use of either initial sizing analytical formulas for pressurized domes or by the use of equilibrium nodal loading from finite element models of low fidelity compared to refined finite element analysis can be significantly underestimated. Some of the implications on CFRP structural sizing at the specified location are developed.

[1]* Corresponding Author: Lecturer / Airframe stress and strength analysis, Centre for Aeronautics, i.giannopoulos@cranfiled.ac.uk
[2] Professor / Mechanics, Department of Mechanics, stathis@central.ntua.gr
[3] Professor / Fatigue and Damage Tolerance, Faculty of Engineering and Computing, ab8295@coventry.ac.uk

Nomenclature

θ, φ	=	spherical coordinate system angular coordinates (rad)
$N\theta\theta$	=	shell element unit force loading along θ direction (N/mm)
$N\varphi\varphi$	=	shell element unit force loading along φ direction (N/mm)
$M\theta\theta$	=	shell element unit moment loading along θ direction (N)
$M\varphi\varphi$	=	shell element unit moment loading along φ direction (N)
$\sigma\theta\theta$	=	shell element normal stress along θ direction (MPa)
$\sigma\varphi\varphi$	=	shell element normal stress along φ direction (MPa)

I. Introduction

Applied stress analysis methodology for aircraft design is based on the elementary theory of structural mechanics. From an airworthiness point of view, the strongest argument for relying upon the results of analytical calculations for structural sizing is the integrity and durability of the components designed that has been validated in service. Metallic materials have been used extensively in the airframe manufacturing for some decades. Most of the today's existing stress analysis methods have emerged through that era. It can be argued that stress analysis methods have been proven airworthy by taking advantage of the specific attributes of the metallic materials, with plasticity being one of them. Currently, there is an increased usage of carbon fiber reinforced plastic (CFRP) materials for aircraft structural primary load-carrying members where the existing methodologies for component sizing have not yet been extensively validated in service. Thus, a question is posed as to whether the same

methods of the past can be assumed reliable for using on structures made of CFRP materials.

Before the extensive finite element modeling for structural analysis, design office procedures for initially assessing the strength of a structural part would primarily rely on analytical methods. The final clearance of the structure would then be justified by a part, a component, and/or by a full-scale structural test. For some decades now, the usage of computational tools provides a discrete, “nodal” loading pattern derived from a “global aircraft finite element (FE) model,” which is basically the means for coarsely distributing the flight and inertial loading to the various structural elements according to their relative stiffness. Rules for the parameters of the numerical model generation are described in company design manuals. Solutions of the numerical global FE model generated under the application of loading cases are in the form of sets of “nodal equilibrium loads.” From that point onward, simplified mechanics would be used to give a representation of the internal structural loading in terms of local stress distributions. Stress analysis in most of the cases relies upon the output nodal loading from a global FE model to further analytically process the applied stress field and evaluate the integrity of the structure. This general aerospace standardized procedure is not a valid one for the structural application under investigation, as will be shown in the following sections.

When greater fidelity in the numerical results is requested, refined finite element models are generated, using more computational nodes. Due to the high computational costs and the limitations in computational power, these models reflect only a smaller part of the complete structure. The study herein is a refined finite element model numerical investigation at the lap joint location between the empennage fuselage structure and a domed end-pressure bulkhead, shown in Figs. 1

and 2. The aim of the study is to provide a better understanding of the structural response and the loading levels at the joint location through the proposed numerical analysis procedure, as well as to provide some context for the implications caused by using CFRP materials for the design of similar structural parts as in contrast to using the more traditional metallic materials.

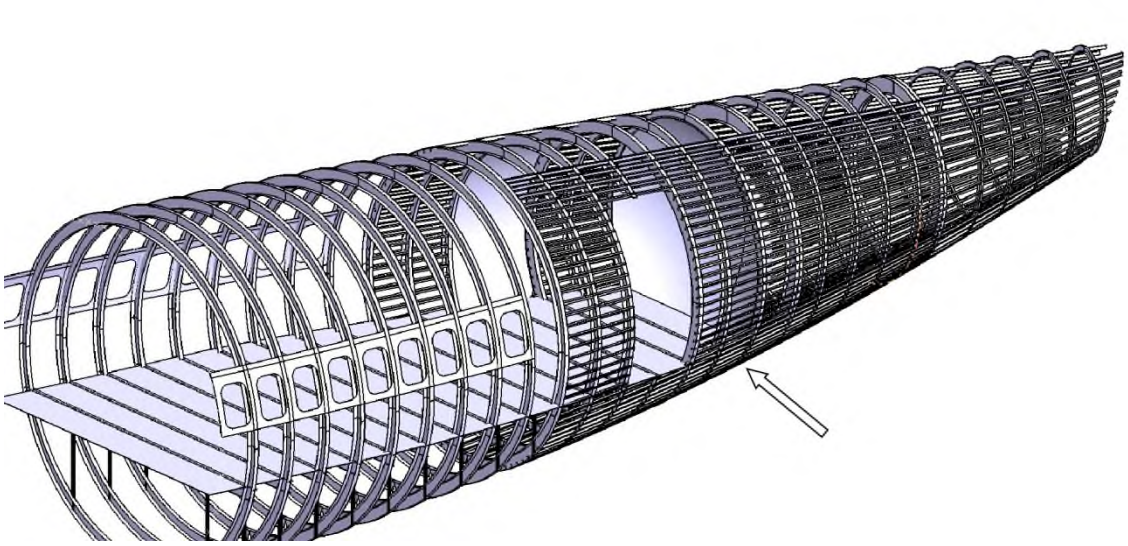

Fig. 1 Conceptual design of an aircraft empennage structure. The airframe location under investigation is indicated.

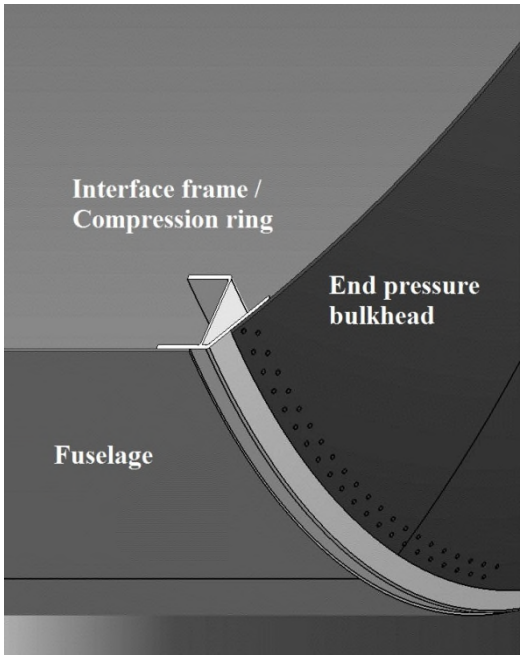

Fig. 2 Enlarged view of the joint between the end-pressure bulkhead dome and the cylindrical fuselage via a frame-type interface structure (compression ring).

Pressurized aircraft vehicle end-fuselage bulkheads are designed either as flat stiffened structures or as dome-shaped ones, stiffened or unstiffened [1]. The dome-shaped structures are usually subjected to limited space requirements. For that reason, they are shaped as part-spherical or part-elliptical ones [2]. These bulkheads are often attached by fasteners to the rest of the structure. The most advantageous stress distribution for an end-pressure bulkhead connected to a cylindrical fuselage under positive internal pressure differential is achieved when the dome is of a half-spherical shape [2]. The biaxial stress in pressurized dome structures is known and documented in the literature.

The scenario of the case study herein investigates the conceptual joint in the empennage of an airframe, shown in Fig. 1. It is assumed that the bulkhead is joined by mechanical fasteners to the last frame (compression ring) of a cylindrical fuselage, shown in Fig. 2. The area under investigation does not take into account possible

bulkhead frames along the meridian direction of the hemisphere that could be joined with fuselage longerons. It addresses the loading of the skin-to-skin lap joint over the bulkhead surface.

Similar studies are not available in the public domain, and some of them are protected by intellectual property rights. A relevant study by Becker and Wacker [3] was performed in the pressure bulkhead of the Ariane-5 tank structure. The bulkhead was made of metallic materials. The focus of the study was the nonlinear numerical investigation including the metallic material plasticity effects. An older and more relevant analytical investigation by Williams [4] highlighted some of the problems of the aircraft pressure cabins. The lack of today's numerical tools provided limited insight to more complex designs. There are various studies [5–13] that considered the analytical and numerical approaches of stresses in vessel-type CFRP structures under pressure. The context of those studies was derived from the aftermath of a different industrial sector and deviates from the one herein, mainly due to considering the vessel-type structures as being monocoque types, which are not implicated by the localized effects of assembled parts with fasteners. The current study is mainly informed from standard airframe design textbooks [1, 2, 14–16].

II. Approach Methodology

A. Deviations from the Elementary Structural Mechanics Theory

Initial structural sizing formulas for pressure dome sizing are found within the literature of structural mechanics [17,18] and are extensively quoted in airframe structural analysis textbooks [14,16]. The stress solution on a pressurized dome surface involves hoop membrane stresses along the meridian and equatorial directions of the spherical surface of equal magnitude. The structural part of the investigation is

a part of a spherical dome under internal pressure. Acceptable stress results are anticipated and compared to the elementary theory ones as long as the parameters of the problem represent the real structure, especially the boundary conditions of it. Figure 3 serves as a demonstration to the aforementioned statement by using the displacement results from FE analysis on a quarter of a dome structure. The pressurized part-semispherical dome in Fig. 3 has its planar periphery constrained in translation along the direction of its axis of revolution and is not tangent to the edge of the surface, as in the elementary problem formulation. The structure under these boundary conditions has a tendency to shrink along its major diameter when pressurized because it is only a part of a hemisphere and not a full one. The result of it is the generation of a complex stress pattern at the boundary of the structure.

A more complicated problem is formulated when the natural tendency of the dome to shrink is internally constrained by assembling it to an elastic fuselage structure, thus incurring reactions perpendicular to the surface. An approximation to the deflected shape of the bulkhead in such a case is depicted in Fig. 4. From the deflected shape, the existence of internal moment loading on the structure laminate is presumed, provided that it has a relative substantial thickness to resist that loading.

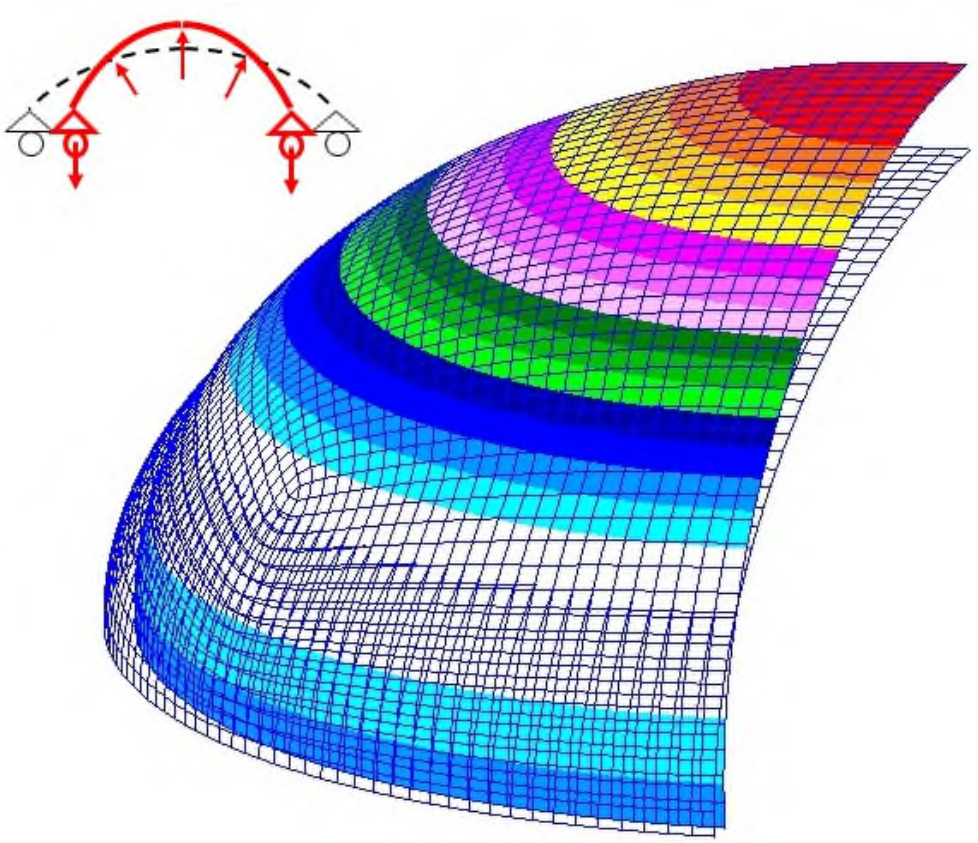

Fig. 3 FE model of a part-hemispherical bulkhead under internal pressure showing the tendency of shrinkage along its major diameter (axis) when the translational degree of freedom along the revolution axis is constrained.

The structural reaction to positive pressure differential is represented by unit loading vectors in a spherical coordinate system, shown in Fig. 5. The loading vectors on the bulkhead structure are tangent to the bulkhead surface along the meridian and equatorial curves. The focus of the investigation lies in the vicinity of the geometrical intersection of the fuselage and the bulkhead, shown in Fig. 2.

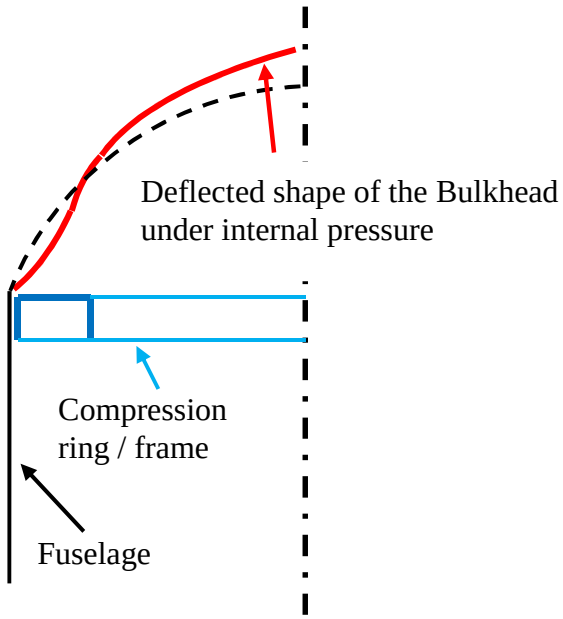

Fig. 4 Sectional representation of the deflected shape of a bulkhead dome under pressure.

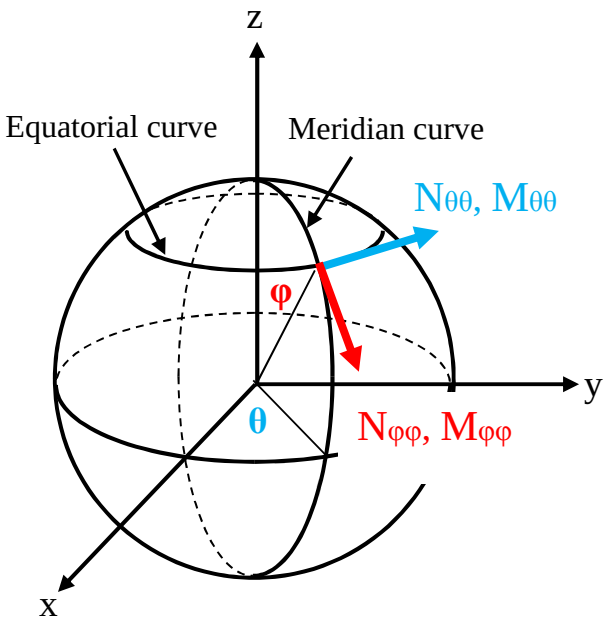

Fig. 5 Spherical coordinate system for vector internal loading representation.

Along the spherical surface equatorial curves and tangent to those, the structural internal loading in terms of force and moment are represented by $N\theta\theta$ and $M\theta\theta$, respectively. $N\theta\theta$ is the hoop reaction to internal pressurization which is tensile for the bigger part of the structure. Approaching the geometrical intersection, it becomes compressive due to the equator's shrinkage effect, as illustrated in Fig. 3. The unit moment load $M\theta\theta$ can be evidenced from the shape of the deflected structure depicted in Fig. 4. The cause for the structural response of Fig. 4 is the counteraction of the fuselage with the compression ring frame to the shrinking effect of the bulkhead along its major diameter. Tracing the spherical surface meridian curves and tangent to those, the internal force and moment loading are represented as $N\varphi\varphi$ and $M\varphi\varphi$, respectively. Unit load $N\varphi\varphi$ is the anticipated tensile hoop reaction to pressure. The unit moment load $M\varphi\varphi$ is the most unobvious loading component and relatively difficult to visualize. It is the result of the axisymmetric pattern of the deflected pattern shown in Fig. 4.

B. Benchmark Test and Comparison of Analytic with FE Results

Modeling a flat plate under pressure, where standard shell-type finite elements (CQUAD4, PSHELL, [19]) are typically and currently used by the airframe design industry, is an element mesh-size-dependent solution [19,14]. A bypass method used to overcome the mesh size dependency in similar problems is to acquire the nodal built in constraint reaction force and moment values from the numerical solution rather than requesting the shell elements stress output from the numerical solver. Consequently, by applying those loads in an analytical fashion at the boundary of the structure, better approximated stress results are generated. When applying this

numerical procedure at the case of a cylindrical fuselage joined to a part-hemispherical dome, the aim of it would be to retrieve the nodal equilibrium force $N_{\varphi\varphi}$ and moment $M_{\theta\theta}$ loading along the intersection curve of the two surfaces. The abrupt change, though, of the surface smoothness at the interface location which joints the geometrical shapes of two different curvatures causes the nodal equilibrium loads at the interface to be element size dependent as well. To study the deviation between the analytic problem formulations of a cylinder connected to a part sphere [17] at the location of the geometrical interface, a series of FE models with variable mesh sizes were constructed and benchmarked against the solution of [17]. Shown in Fig. 6, are three of the variable mesh-sized FE models built in NASTRAN that were used for benchmarking. The benchmark took place on the simpler geometrical model of a cylindrical surface connected to the part-spherical dome for the reason that the analytic solution of it is available in the literature. That model does not contain the complication of an additional circumferential frame along the intersection of the surfaces, which is present in the actual airframe structure under investigation. The benchmark showed a difference of 40% in the magnitude $M_{\theta\theta}$ between the coarse and the refined models of Fig. 6. This result led to the conclusion that the only way of resolving the true loading state at that interface in terms of $M_{\theta\theta}$ was through extrapolation of the nodal results from models of varied element sizes. Summarizing, by using the currently aerospace standard finite element formulations at the intersection curve of a cylinder to a part-spherical surface, not only stress output results are element size dependent but nodal moment $M_{\theta\theta}$ loads as well.

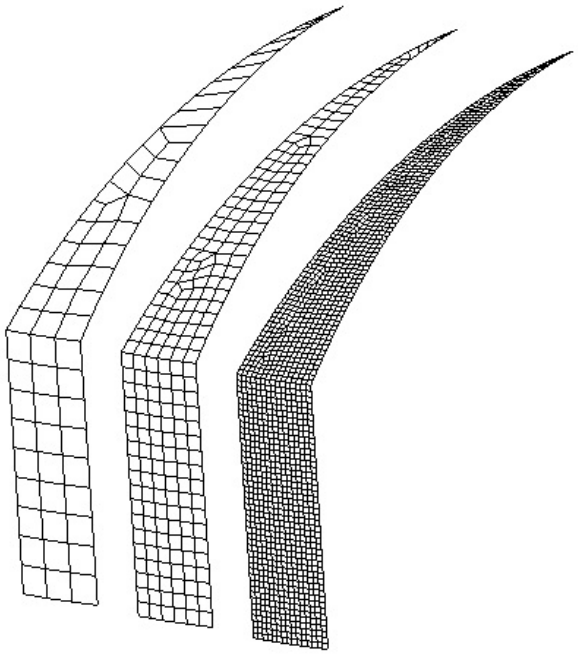

Fig. 6 Models of various refinement for comparison with the analytical solution of the nodal equilibrium force and moment at the intersection curve between the cylindrical and dome structure.

C. Case Study Conceptual Structure and Finite Element Model

The conceptual structure of the investigation consisted of a part-hemispherical bulkhead shell of 2.5 m radius, attached to a 3-m-diam fuselage using an interface frame. In this study, there were no supporting frames to the bulkhead skin along the meridian direction. Alternatively, in the case where the conceptual design incorporated frames along the meridian direction, these would prevent excessive skin distortion at the frame support location and maximum skin distortion would be present in the unsupported region in between the frames.

Both the fuselage and the bulkhead structures were assumed to be made of CFRP materials. The interface compression ring frame, shown in Fig. 2, was made of aluminum. The CFRP material system was Tenax-J HTS40 E13 3K 200 TEX woven fibers impregnated with MTM45-1 resin with a cured ply thickness of 0.2 mm.

Elastic moduli along the principle directions were assumed identical and equal to 60 GPa. The bulkhead laminate had a quasi-isotropic layup configuration of 2.4 mm total thickness. The manufacturing layup process is shown in Fig. 7, where, basically, ply stripes were laid over the bulkhead surface. The layer stripe width had been calculated for avoiding excessive fiber direction deviation due to draping. The internal pressure differential was 0.09 MPa.

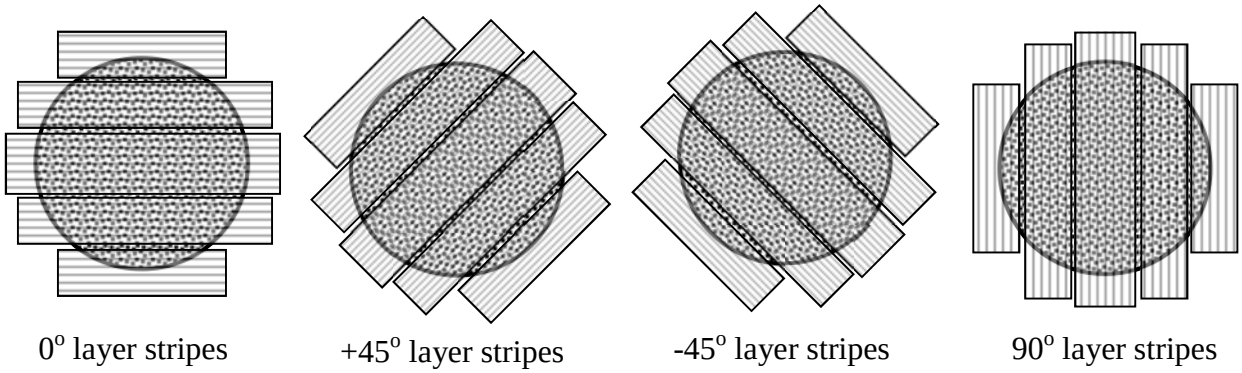

Fig. 7 Domed skin surface layup from preimpregnated CFRP layers.

The local model of the joint generated in NASTRAN is shown in Fig. 8. Shell elements (CQUAD4, MAT8, PCOMP [19]) were chosen to represent the thin-walled shell structure. This element technology is currently the aerospace standard for global FE aircraft numerical modeling. The benchmarking, explained previously in Sec. II.B, was performed in order to assess the finite element output result accuracy in terms of unit nodal force and unit moment equilibrium loading. The result of the benchmarking dictated the appropriate element size needed for the case study to achieve satisfactory results within a specified tolerance. Only a sector of the fuselage was modeled, as shown in Fig. 8. Axisymmetric boundary conditions were defined along the section boundary, and internal pressure was applied on the shell elements.

Results are drawn in terms of loading from the intersection curve with the cylindrical part and for 300 mm inboard along the bulkhead surface; see Fig. 8. The numerical analysis performed was nonlinear static (SOL400).

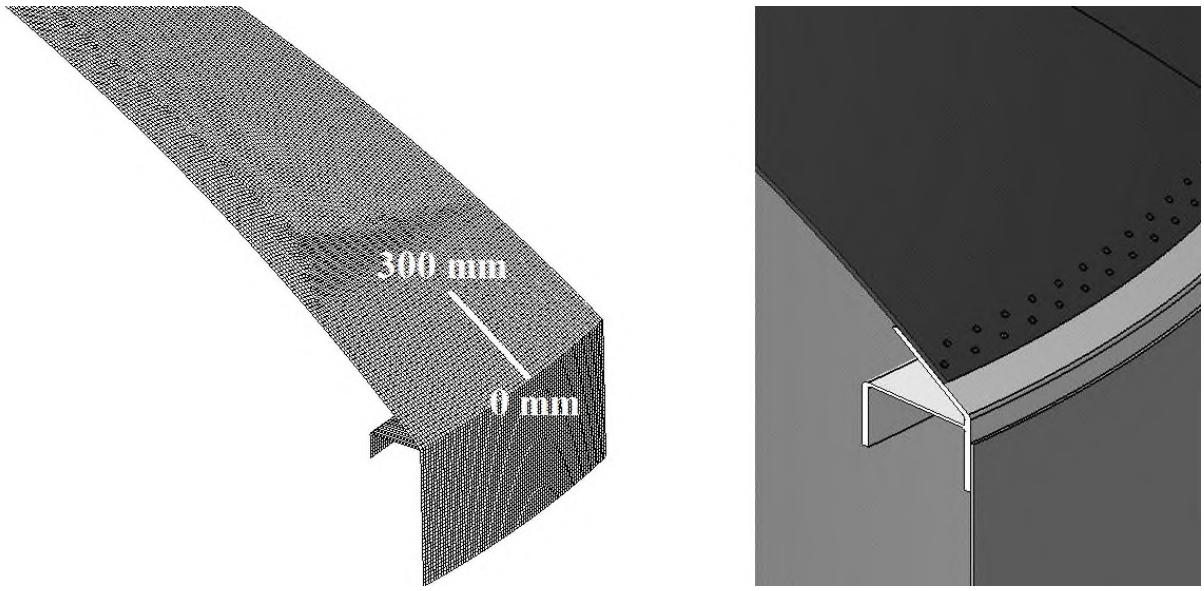

Fig. 8 FE model mesh used for deriving the loading in the vicinity of the interface for the case study. Loading results are analyzed for the distance shown (0–300 mm).

III. Results

In Fig. 9, a pictorial representation of the defined unit force and moment loading is shown. In Fig. 10, the resulting internal loading from the FE calculation is presented for a distance of 300 mm from the geometrical intersection as per Fig.8.

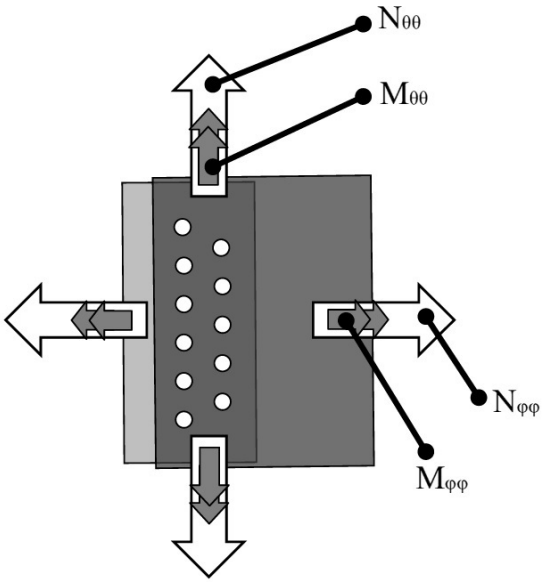

Fig. 9 Definition of the force and moment unit loading vectors on an elementary sector of the bulkhead interface lap joint.

The meridian unit force loading $N_{\varphi\varphi}$ (Fig. 10a) after 250 mm from the geometrical intersection attained the anticipated magnitude from the initial sizing analysis of spherical domes under pressure [17]. For the structure under study, the variation of the magnitude of the meridian force was less than 15% for the complete analysis length. The loading remained tensile for the whole region under investigation.

Moment unit loading $M_{\varphi\varphi}$ (Fig. 10b) could not be predicted from elementary theory of spherical domes under pressure. For the case study, the magnitude of the vector had a peak at the surface intersection location. After approximately 250 mm, it diminished to zero; whereas past 150 mm from the intersection, it was less than 15% of the maximum value. The sign of the moment shifted from positive to negative at around 50 mm from the interface, following the change in the dome's deflected shape, shown in Fig. 4.

The tangential-force unit loading $N\theta\theta$ (Fig. 10c) was initially negative until 100 mm from the geometrical intersection. Following that distance and after 150 mm approximately, it gradually rises to the anticipated elementary theory value.

The tangential moment unit loading $M\theta\theta$ (Fig. 10d) changes its sign from positive to negative at approximately 50 mm from the interface location, following a similar change to the meridian moment. After 250 mm, the magnitude of the moment is practically zero, whereas at 150 mm, its value has diminished to more than 15% of the maximum at the interface location.

a) Unit force tangent to meridian curves, $N_{\varphi\varphi}$

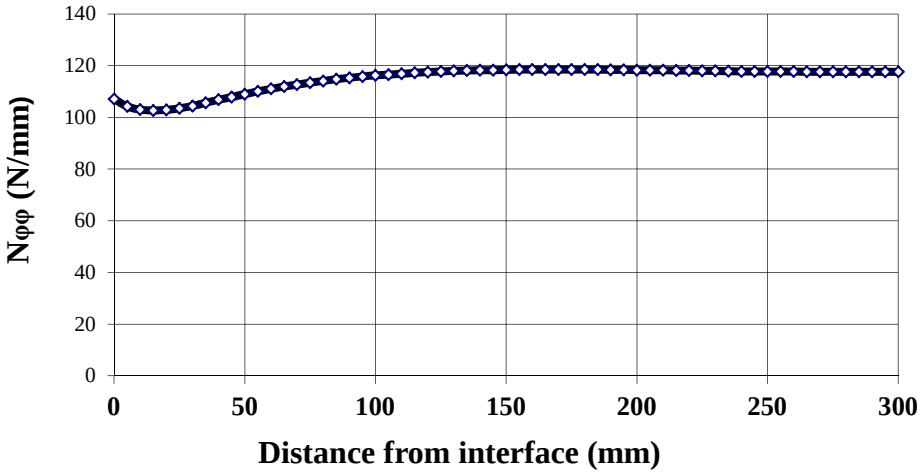

b) Unti moment tangent to meridian curves, $M_{\varphi\varphi}$

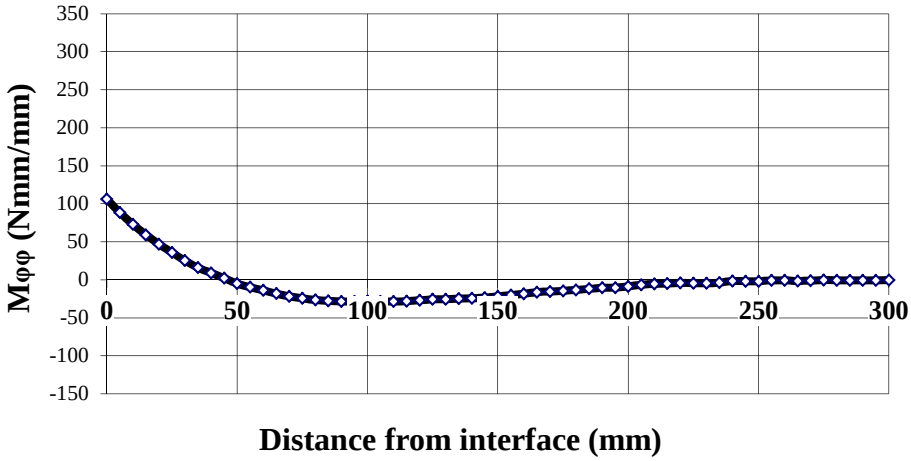

c) Unit force tangent to equatorial curves, $N_{\theta\theta}$

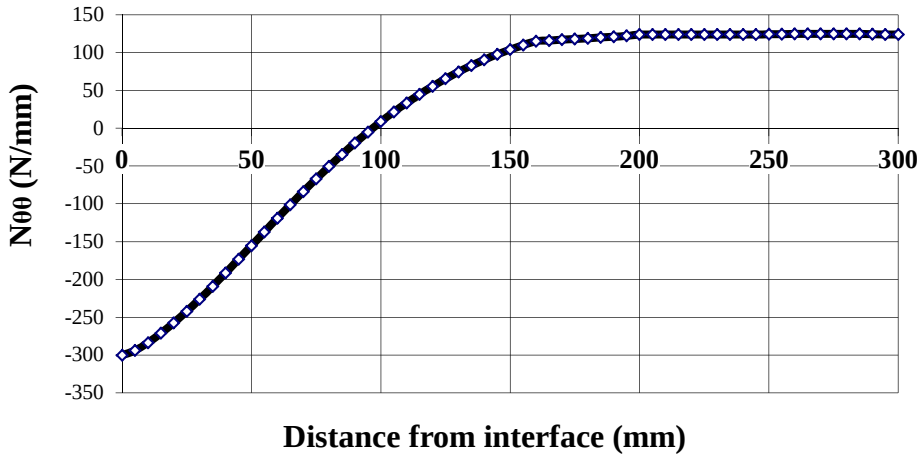

d) Unit moment tangent to equatorial curves, $M_{\theta\theta}$

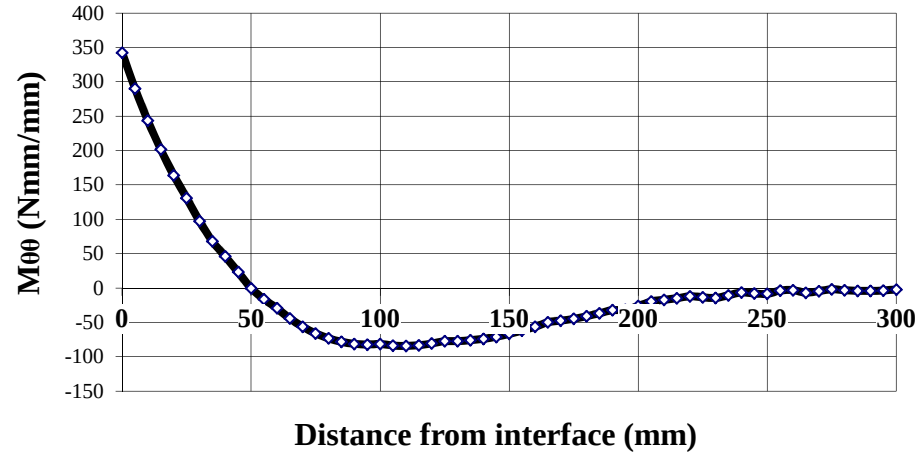

Fig. 10 Internal unit force and moment loading along a meridian curve over the bulkhead skin surface from the interface position to 300 mm towards the apex of the bulkhead dome (Fig. 8).

Practically, approximately past the 250 mm distance from the geometrical intersection of the bulkhead with the fuselage surface, the internal loading stress tensor was described by tensile hoop stresses along the meridian and equatorial directions, and tangent to those. Before that distance, which is considered to be the

vicinity to the geometrical intersection, high compressive loads existed along the equatorial direction and there was an equally alarming increase in the moment loading in both principle directions as well. Loading vectors $N_{\varphi\varphi}$ and $M_{\theta\theta}$ along the intersection curve were benchmarked in Sec. II.B, and results can be regarded as acceptable for the FE mesh size generated. The rest of the results are finite element technology dependent, and thus could only be verified by real-life testing.

Evaluation of the stresses on the lamina level was performed following the assumptions of the classical lamination theory (CLT) [20,21], making use of the unit loading state of Fig. 10. One thing to point out is that there is a variance in the perception of the laminate's layup configuration, depending on the location of the observer around the structure's periphery, shown in Fig. 11. To illustrate the previous statement with an example, the CFRP layer shown in Fig. 11 includes the black- and white-striped blocks laid over the top view of the domed bulkhead, and it is supposed to have its principle fiber direction parallel to the stripes. While moving around the periphery of the bulkhead, this same layer is perceived as a 0 deg layer at position a, as a 45 deg layer at position *b*, and as a 90 deg layer at position *c*. Stresses resulting from unit force and moment loading are affected by this variable layup perception.

To generate the resulting laminate stresses upon the application of the unit loading of Fig. 10, a simple demonstration follows by applying the loading over a homogeneous isotropic material with an elasticity modulus of E = 60 GPa and a Poisson ration of ν = 0.3. Results at three different locations on the bulkhead surface at the vicinity of the joint are displayed in the following:

Past a distance of 250 mm from the geometrical intersection, moments $_{M\theta\theta}$ and $_{M\varphi\varphi}$ were equal to zero (Figs. 10b and 10d). The supposed isotropic bulkhead shell reacted to the internal pressurization with bidirectional hoop stresses:

$$N_{\varphi\varphi} = N_{\theta\theta} = 118 \text{ N/mm (Figs. 10a and 10c) =>}$$

$$\sigma_{\varphi\varphi} = \sigma_{\theta\theta} = 50 \text{ MPa}$$

Neglecting the bidirectional moment and assuming the worst compressive $_{N\theta\theta}$ superimposed by $N_{\varphi\varphi}$ loading, then the maximum stresses on the assumed isotropic bulkhead skin at the edge of the skin were the following (Figs. 10a and 10c):

$$N_{\varphi\varphi} = 107 \text{ N/mm}, N_{\theta\theta} = -300 \text{ N/mm =>}$$

$$\sigma_{\varphi\varphi} = 45 \text{ MPa}, \quad \sigma_{\theta\theta} = -125 \text{ MPa}$$

Summing the effect of the bidirectional unit loading with the bidirectional moment vectors at the edge of the assumed isotropic skin (Figs. 10a–10d),

$$N\varphi\varphi = 107 \text{ N/mm}, \quad N\theta\theta = -300 \text{ N/mm},$$

$$M\varphi\varphi = 110 \text{ N}, M\theta\theta = 350 \text{ N =>}$$

$$\sigma_{\varphi\varphi max} = 160 \text{ MPa}, \sigma_{\varphi\varphi min} = -70 \text{ MPa},$$

$$\sigma_{\theta\theta max} = 239 \text{ MPa}, \sigma_{\theta\theta min} = -490 \text{ MPa}$$

Following the preceding simple demonstration, we applied the last, which is worst-case loading scenario on the CFRP laminate of our case study. The layup configuration, taking into account Fig. 11, is perceived as [0/90, +/-, 90/0, 0/90, +/-, -/+] sat position a and as [+/-, 90/0, -/+, +/-, 90/0, 0/90] s at position b. The maximum results were calculated at the midply position of each layer:

At position a of Fig. 11, along the periphery and at the tip of the intersection,

$N\varphi\varphi$ = 107 N/mm, $N\theta\theta$ = -300 N/mm,

$M\varphi\varphi$ = 110 N, $M\theta\theta$ = 350 N =>

$\sigma_{\varphi\varphi max}$ = 170 MPa, $\sigma_{\varphi\varphi min}$ = -182 MPa,

$\sigma_{\theta\theta max}$ = 188 MPa, $\sigma_{\theta\theta min}$ = -567 MPa

At position b of Fig. 11, along the periphery and at the tip of the intersection,

$N\varphi\varphi$ = 107 N/mm, $N\theta\theta$ = -300 N/mm,

$M\varphi\varphi$ = 110 N, $M\theta\theta$ = 350 N =>

$\sigma_{\varphi\varphi max}$ = 162 MPa, $\sigma_{\varphi\varphi min}$ = -202 MPa,

$\sigma_{\theta\theta max}$ = 218 MPa, $\sigma_{\theta\theta min}$ = -597 MPa

From the preceding shown stress evaluations, it is evident that the numerically calculated loading state can be underestimated if the effects of the boundary conditions are not taken properly into account.

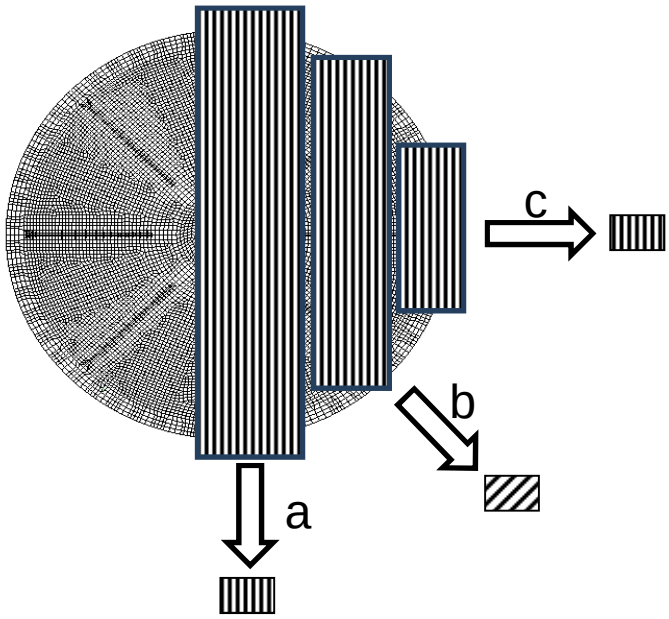

Fig. 11 Variance in the perception of the bulkhead laminate layup configuration depending on the observer location around the periphery.

IV. Discussion

Depending on the specific design, materials, and geometric configuration, there is a specific distance from the geometrical intersection between a cylindrical fuselage and a part-semispherical dome, where the loading is variable to the distance and is far greater than the bidirectional hoop stresses on a pressurized sphere. The severity of the results of such a loading condition could be overshadowed since, most of the time, the connection between the compression ring frame and the pressure bulkhead is more complicated in terms of structural arrangement, creating a secure distance between the bulkhead and the geometrical inflection point of the interface [13,16].

One of the major differences in the airworthiness structural clearance approach between a metallic and a CFRP structure is the structural testing evidence required.

This mainly results from the relatively smaller existing field experience and strength validation of the CFRP structures as opposed to the metallic ones. Clearance directives dictate that the strength and fatigue life of the CFRP structure in a damaged state has to be verified by testing. Composite laminated structures containing damage in the form of interlaminar delaminated regions are susceptible to failure under compression loads. Our analysis has indicated the existence of high compressive loading in the vicinity of the joint. In such cases, besides the elastic instability problems that could arise in thin-walled structures irrespective of the material used, the CFRP laminate also has to be sized against its compression after impact (CAI) strength [15]. CAI strength depends on numerous factors and effectively results from component tests, which have to be performed early in the design stage for use in material selection and qualification.

In the case study, the compression ring was designed by metallic materials. In such a scenario, the designer could avoid the area of high-intensity loading by effectively offsetting the CFRP bulkhead structure further inboard. The advantage of such a design was to expose the metallic part of the lap joint to the transitional high loading area, which is easier to inspect and has a more extensively validated and documented strength, fatigue, and damage-tolerance properties.

There is also an opportunity to place the fastener arrays within the region of the tangential-force loading sign change, and thus decrease the effect of the biaxial loaded laminate in case it is found that most favorable strength results can result. The lap joint assembly with fasteners is shown in Fig. 2. At a distance of approximately 100 mm from the intersection, as shown in Fig. 10c, the compressive load equals to zero. Effectively, at the region of the tangential-force loading sign change, the lap joint laminate is almost uniaxially loaded with relatively reduced biaxial moment

vector magnitudes. A typical lap joint test specimen could be used for substantiating the structural strength at that location, provided that the applied loading besides the unidirectional tension along the meridian is assumed negligible; else, the loading on the transitional area has to be assessed by a fine finite element mesh in a conservative manner and the effects of the biaxially loaded fastener holes and the fastener bearing have to be superimposed on the laminate loading.

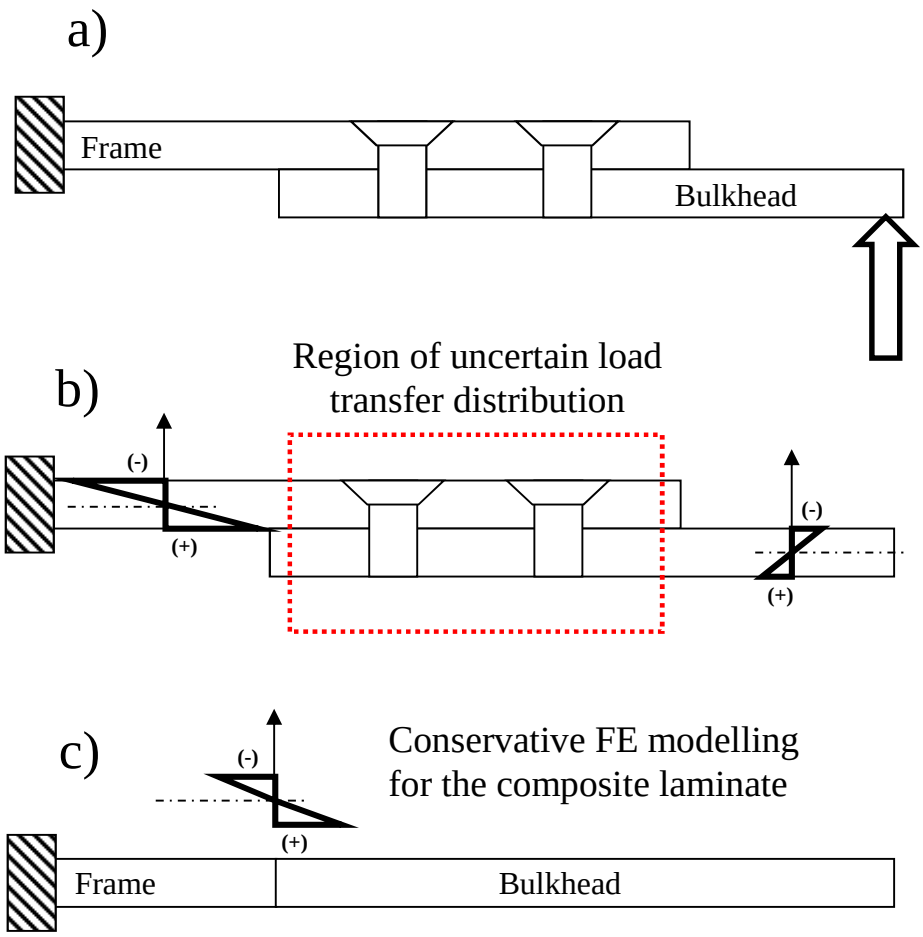

Fig. 12 a) Beam model lap joint, b) region of uncertain laminate loading transfer, and c) exposure of the structure to a lengthier and a more severe end loading.

For sizing the lap joint effectively, the bidirectional force and moment loading of the area under investigation need to be evaluated. A conservative FE modeling approach to that shown in Fig. 12 would be to assume that the CFRP laminate is

modeled to the edge of the structure, thus being exposed to the complete variation of the loading field. That elementary loading in terms of unit force and moment, shown in Fig. 10, applied on a laminate section following the CLT assumptions would result in the loading of the individual composite material layers [20,21]. It is usual for the finite element modeling practice to exclude the presence of fasteners in the idealization of joints in order to avoid unnecessary modeling effort spent on fastener hole stress concentrations, fastener fits and pretightening, contact, three-dimensional effects of laminates, etc. A usual and preferred approach is to solve for the laminate loading and superimpose on top of it the stress field caused by the presence of holes and fastener bearing loads. Another perspective for the modeling approach of Fig. 12 is the exposure of the edge of the laminate to higher-intensity loading, in order to assess the through-the-thickness edge stresses caused by the in-plane loading in a more conservative manner.

Full-scale testing is used for satisfying the airworthiness structural clearance procedures. Only full-scale testing can generate the actual loading situation and assess the structural integrity of the joint. Ideally, correlation with full-scale test results from structural testing could verify or amend the aforementioned case study numerical results. Testing data of full-scale pressure bulkhead tests are difficult to come across. If, in the future test, data become available in the public domain, the present study can further progress. Nonetheless, the previously proposed numerical modeling approach, which is based on the currently standard FE technology used in the aerospace industry along with the discussed design complications, can provide designers of similar structural interfaces with an insight to the complications that arise and attain a better initial estimation of the expected structural response.

V. Conclusions

The numerical investigation of the conceptual joint between a fuselage and a pressure bulkhead has revealed the following:

1) Numerical results from coarse FE analysis in terms of loading should not be used for sizing in similar structural arrangements, unless the finite element formulation provides acceptable results in a benchmarking procedure similar to Sec. II.B. Refined mesh FE results can be employed for deriving the applied loading for initial design purposes, but attention has to be drawn to the fact that not only the stress results along the geometrical interface are mesh size dependent but also the force and moment nodal values.

2) High-intensity loading exists in the vicinity of the geometrical intersection where the joint was assumed; see Fig. 10. The existing force and moment loading magnitudes, as calculated by the FE analysis, cannot be predicted by the use of elementary structural analysis or coarse meshed FE models. The structural response responsible for the high-intensity loading in the vicinity of the joint is attributed to the fact that the major diameter of the bulkhead has a tendency to shrink upon pressure under the boundary conditions imposed by the rest of the structure; see Fig.4.

3) The numerical analysis has shown the existence of high compressive loading in the vicinity of the joint: a loading mode that affects CFRP structures more than structures made of metallic materials. Besides the elastic instability considerations, the compression after impact strength has to be taken into account.

4) Stress results are affected by the stress concentrations of the fastener holes and the edge stress raising effects of the CFRP laminate. In the vicinity of the tangential load, with $N_{\theta\theta}$ being close to zero (Fig. 10, where the bidirectional moments

are reduced as well), opportunities for optimal placement of the fastener pattern and/or the edge of the bulkhead on the assembly exist. This design option can be achieved by a wider interface frame flange and a smaller peripheral radius bulkhead; see Fig. 2.

5) There are various design and analysis challenges posed by the application of CFRP materials, and they need to be faced until a final airworthiness structural qualification is achieved. By the aforementioned numerical procedure, better approximated stress results could be incorporated earlier within the design cycle of the product and provide the insight needed for decision making in terms of material selection and structural design configuration.

References

[1] Howe, D., Aircraft Loading and Structural Layout, AIAA Educational Series, AIAA, Reston, VA, 2004, p. 457.

[2] Niu, M. C. Y., Airframe Structural Design, Hong Kong Conmilit Press, Hong Kong, 1995, pp. 398–402

[3] Becker, W., and Wacker, T., "Comparison Between Test and Analysis of a Tank Bulkhead Loaded in the Plastic Range," Aerospace Science and Technology, Vol. 1, No. 1, 1997, pp. 77–81. doi:10.1016/S1270-9638(97)90025-0

[4] Williams, D., "Structural Problems of Aircraft Pressure Cabins," Progress in Aeronautical Sciences, Vol. 1, Pergamon, New York, 1961, pp. 206–237.

[5] Hyer, M. W., and McMurray, J. M., "Internally Pressurized Elliptical Composite Cylinders," Composite Structures, Vol. 46, No. 1, 1999, pp. 17–31. doi:10.1016/S0263-8223(99)00038-0

[6] Krikanov, A. A., "Composite Pressure Vessels with Higher Stiffness," Composite Structures, Vol. 48, Nos. 1–3, 2000, pp. 119–127. doi:10.1016/S0263-8223(99)00083-5

[7] Kabir, M. Z., "Finite Element Analysis of Composite Pressure Vessels with a Load Sharing Metallic Liner," Composite Structures, Vol. 49, No. 3, July 2000, pp. 247–255. doi:10.1016/S0263-8223(99)00044-6

[8] Onder, A., Sayman, O., Dogan, T., and Tarakcioglu, N., "Burst Failure Load of Composite Pressure Vessels," Composite Structures, Vol. 89, No. 1, 2009, pp. 159–166. doi:1016/j.compstruct.2008.06.021

[9] Vasiliev, V. V., Krikanov, A. A., and Razin, A. F., "New Generation of Filament Wound Composite Pressure Vessels for Commercial Applications," Composite Structures, Vol.62, Nos. 3–4,2003, pp. 449–459. doi:10.1016/j.compstruct.2003.09.019

[10] Hyer, M. W., and Vogl, G. A., "Response of Elliptical Composite Cylinders to a Spatially Uniform Temperature Change," Composite Structures, Vol. 51, No. 2, 2001, pp. 169–179. doi:10.1016/S0263-8223(00)00142-2

[11] Zhang, Q., Wang, Z. W., Tang, C. Y., Hu, D. P., Liu, P. Q., and Xia, L. Z., "Analytical Solution of the Thermo-Mechanical Stresses in a Multi-Layered Composite Pressure Vessel Considering the Influence of the Closed Ends," International Journal of Pressure Vessels and Piping, Vol. 98, Oct. 2012, pp. 102–110. doi:10.1016/j.ijpvp.2012.07.009

[12] Wang, Y., Zheng, Z., Sun, M., and Zhu, S, "Finite Element Modelling of Carbon Fibre Reinforced Polymer Pressure Vessel," International Conference on Educational and Network Technology (ICENT), IEEE Publ., Piscataway, NJ, 2010, pp. 259–262. doi:10.1109/ICENT.2010.5532177

[13] Adali, S., Summers, E. B., and Verijenko, V. E., "Optimization of Laminated Cylindrical Pressure Vessels Under the Strength Criterion," Composite Structures, Vol. 25, Nos. 3–4, 1993, pp. 305–312. doi:10.1016/0263-8223(93)90177-R

[14] Niu, M. C. Y., Airframe Stress Analysis and Sizing, 2nd ed., Hong Kong Conmilit Press, Hong Kong, 1999, pp. 181–203.

[15] Niu, M. C. Y., Composite Airframe Structures, Hong Kong Conmilit Press, Hong Kong, 1995, pp. 424–429.

[16] Bruhn, E. F., Analysis and Design ofFlight Vehicle Structures, Tri-State Offset, Steubenville, OH, 1973, pp. A16.1–A16.10.

[17] Young, C. Y., and Budynas, G. R., Roark's Formulas for Stress and Strain, 7th ed., McGraw–Hill, New York, 2002, pp. 553–591, 643–644.

[18] Timoshenko, S., Strength ofMaterials Part II, 2nd ed., D. Van Nostrand Company, Inc., New York, 1947, pp. 159–173.

[19] NASTRAN Quick Reference Guide, MSC Software Corp., Newport Beach, CA, 2012.

[20] Reddy, J. N., Mechanics of Laminated Composites Plates and Shells: Theory and Analysis, 2nd ed., CRC Press, London, 2004, pp. 112–129.

[21] Daniel, I., and Ishai, O., Engineering Mechanics of Composite Materials, Oxford Univ. Press, New York, 1994, pp. 142–181.